Int. J. Heat Mass Transfer. Vol. 27, No. 3, pp. 337–349, 1984
Printed in Great Britain

0017–9310/84 $3.00 + 0.00
Pergamon Press Ltd.

NATURAL CONVECTION BETWEEN HORIZONTAL CONCENTRIC CYLINDERS FILLED WITH A POROUS LAYER WITH INTERNAL HEAT GENERATION

P. VASSEUR, T. HUNG NGUYEN, L. ROBILLARD and V. K. TONG THI
Department of Civil Engineering, Ecole Polytechnique, C.P. 6079, Succursale "A", Montreal, Quebec H3C 3A7, Canada

(*Received* 3 *March* 1983 *and in revised form* 13 *June* 1983)

Abstract—The problem of natural convection in an annular porous layer with internal heat generation is studied numerically. At low Rayleigh numbers, a more or less parabolic temperature profile is established across the annulus, resulting in two counter-rotating vortices in each half cavity. Under the effect of weak and moderate convection, the maximum temperature within the porous medium can be considerably higher than that induced by pure conduction. At high Rayleigh numbers, both analytical and numerical analyses reveal a flow structure consisting of a thermally stratified core and two boundary layers with a thickness and heat transfer rate of the order of $Ra^{-1/3}$ and $Ra^{1/3}$, respectively.

NOMENCLATURE

- d' pore diameter [m]
- Da Darcy number, K/L^2
- F coefficient appearing in the definition of the inertial parameter, equation (A1)
- $\mathbf{g}$ gravitational acceleration [m s^{-2}]
- k thermal conductivity of the saturated porous medium [W m^{-1} K^{-1}]
- K permeability of the porous medium [m^2]
- L characteristic length of the porous medium [m]
- n porosity of porous medium
- Nu normalized Nusselt number, defined by equation (25)
- Pr Prandtl number, ν/α
- p dimensionless pressure, $p'K(\rho c)_f/\mu k$
- Q dimensionless heat flux across a unit angle
- r dimensionless coordinate, r'/r_i'
- R radius ratio, r_o'/r_i'
- Ra internal Rayleigh number, $Kg\beta r_i'^3 S'(\rho c)_f/\nu k^2$
- Re Reynolds number based on the characteristic length L, $V'L/\nu$
- Re^* Reynolds number based on the pore diameter, $V'd'/\nu$
- S' volumetric heat generation rate [W m^{-3}]
- t dimensionless time, $t'k/r_i'^2(\rho c)_p$
- T dimensionless temperature, $(T' - T_w')k/(S'r_i'^2)$
- ΔT characteristic temperature difference [°C]
- U' characteristic velocity [m s^{-1}]
- $\mathbf{V}$ dimensionless velocity, $\mathbf{V}'r_i'(\rho c)_f/k$.

Greek symbols

- α thermal diffusivity of the saturated porous medium [m^2 s^{-1}]
- β thermal expansion coefficient [K^{-1}]
- η stretched variable, defined by equation (21)
- μ dynamic viscosity of fluid [kg m^{-1} s^{-1}]
- ν kinematic viscosity of fluid [m^2 s^{-1}]
- ρ density of fluid [kg m^{-3}]
- $(\rho c)_f$ specific heat capacity of the fluid [J m^{-3} K^{-1}]
- $(\rho c)_p$ heat capacity of the saturated porous medium [J m^{-3} K^{-1}]
- π_d boundary parameter, $Pr^2\, Da/n$
- π_i inertial parameter, $nF\, Re\, \sqrt{Da}$
- ϕ angular coordinate
- ψ dimensionless stream function, $\psi'(\rho c)_f/k$.

Superscripts

- $'$ dimensional variables
- $*$ quantities in the boundary layer regime
- $\bar{}$ average value.

Subscripts

- c pure conduction
- i value on inner cylinder
- max maximum value
- min minimum value
- o value on outer cylinder
- r value at reference temperature T_r'
- w value at boundary.

INTRODUCTION

NATURAL convection in enclosed spaces with internal heat generation is of possible importance in the problems of radioactive waste heat removal, electrolytic processes, geothermal energy recovery, nuclear fusion and exothermic chemical reactions, etc.

The problem of natural convection of a heat generating fluid contained in a cavity has been considerably studied in the past. Theoretical and experimental results have been obtained for rectangular cavities [1–3], spheres and vertical cylinders [4], spherical annulus [5] and segments of a sphere [6], subjected to a variety of boundary conditions.

For the problem of a porous medium with internal heat generation, most of the works dealt with the case of

a horizontal layer. For example, Gasser and Kazimi [7] studied the onset of convection in a porous layer with both stabilizing and destabilizing temperature gradients, using the linear stability theory, while Tveitereid [8] used the Galerkin method to solve the heat transfer problem for a porous layer with an adiabatic lower surface. Recently, Somerton *et al.* [9] obtained solutions for the case of a volumetrically heated porous layer with an adiabatic lower surface and a zero applied temperature gradient, using a mixed finite difference–Galerkin method.

In this paper, we present a numerical study of two-dimensional (2-D) laminar convection in a porous medium with uniformly distributed energy sources, and confined between two horizontal concentric isothermal cylinders. The finite-difference method is used to solve the 2-D Darcy–Oberbeck–Boussinesq equations. Solutions for the temperature and flow fields are presented in the form of isotherm and streamlines. Maximum and average temperatures of the fluid layer as well as the heat transfer rates are studied in terms of the two governing parameters R, the radius ratio, and Ra, the internal Rayleigh number, within the range $1 < R \leqslant 4$ and $0 < Ra < 10^4$.

BASIC EQUATIONS

The problem under consideration is that of 2-D steady laminar convection in a porous layer bounded by two horizontal concentric cylinders, as shown in Fig. 1. The porous layer is isotropic, homogeneous and saturated with an incompressible fluid. Both cylinders are maintained at constant equal temperatures while heat is generated by a uniformly distributed energy source within the cavity. This internal heat generation creates a temperature gradient across the layer, and thereby provides a driving mechanism for the natural convection within the cavity.

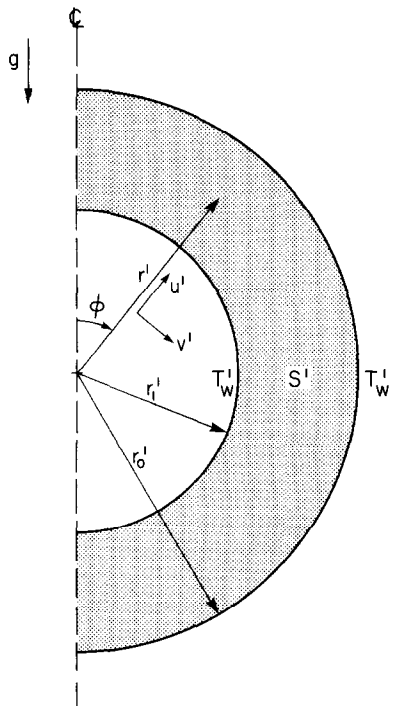

FIG. 1. Flow geometry and coordinate system.

In the present study, the saturated porous medium will be treated as a continuum, with the solid and fluid phases in local thermodynamic equilibrium. Also, the saturating fluid and the porous matrix are supposed incompressible, and all physical properties of the medium, except the fluid density that gives rise to the buoyancy force, are taken to be constant. Finally, the fluid motion is assumed slow enough for the inertial force to be small compared to the buoyancy, and the diffusion of vorticity from a boundary to be negligible (the validity of these approximations is discussed in the Appendix). The fluid motion then obeys the well-known Darcy–Oberbeck–Boussinesq equations [9]. For the case of volumetric heating considered here, the governing equations can be written as

$$\nabla \cdot \mathbf{V}' = 0, \tag{1}$$

$$\mathbf{V}' = \frac{K}{\mu}(\rho' \mathbf{g} - \nabla p'), \tag{2}$$

$$(\rho c)_p \frac{\partial T'}{\partial t'} + (\rho c)_f (\mathbf{V}' \cdot \nabla) T' = k \nabla^2 T' + S', \tag{3}$$

$$\rho' = \rho_r' [1 - \beta (T' - T_r')], \tag{4}$$

where $\mathbf{g}$ is the gravitational acceleration, $\mathbf{V}'$, p', T', ρ', μ and $(\rho c)_f$ are the filtration velocity, pressure, temperature, density, viscosity, and heat capacity of the fluid, respectively. K is the permeability of the saturated porous medium, S' is the rate of internal heat generation, β is the thermal expansion coefficient, and $(\rho c)_p$ and k are the heat capacity and the effective thermal conductivity of the porous medium.

For the case of 2-D flow, the above equations can be reduced to the following coupled differential equations for the stream function and temperature:

$$\nabla^2 \psi = Ra \, \mathscr{L}(T), \tag{5}$$

$$\frac{\partial T}{\partial t} + (\nabla \cdot \mathbf{V} T) = \nabla^2 T + 1, \tag{6}$$

where

$$\mathscr{L}(T) \equiv \left(\sin \phi \frac{\partial}{\partial r} + \cos \phi \frac{\partial}{r \partial \phi} \right) T, \tag{7}$$

and $Ra = K g \beta r_i'^3 S' (\rho c)_f / \nu k^2$ is defined as an internal Rayleigh number. Equations (5) and (6) have been made dimensionless by scaling time, length velocity and temperature with $(\rho c)_p r_i'^2/k$, r_i', $k/r_i'(\rho c)_f$ and $S' r_i'^2/k$, respectively.

As a result of the symmetry across the vertical axis $\phi = 0$, we shall have to solve the above equations in the half cavity $1 \leqslant r \leqslant R$, $0 \leqslant \phi \leqslant \pi$, subject to the following boundary conditions

$$\psi = T = 0 \quad \text{for} \quad r = 1, R; \quad 0 \leqslant \phi \leqslant \pi, \tag{8}$$

$$\psi = \frac{\partial^2 \psi}{\partial \phi^2} = \frac{\partial T}{\partial \phi} = 0 \quad \text{for} \quad \phi = 0, \pi; \quad 1 \leqslant r \leqslant R. \quad (9)$$

Condition (8) corresponds to the case of inner and outer cylinders both impermeable and maintained at the same temperature. Condition (9) simply expresses the symmetry across the vertical axis.

ANALYSIS

Before discussing the results obtained by numerical calculations, it is instructive to examine the general features of the velocity and temperature fields in the limits of very small or very large Rayleigh numbers, corresponding to the pseudo conduction and boundary layer flow regimes, respectively.

The pseudo conduction regime

For small Rayleigh numbers, the fluid motion is weak, the heat transfer is mainly due to conduction, and the steady-state temperature and flow field can be described by equations (5) and (6) with the nonlinear convective term neglected, i.e.

$$\nabla^2 T + 1 = 0, \quad (10)$$

$$\nabla^2 \psi = Ra\, \mathscr{L}(T), \quad (11)$$

which, under the boundary conditions (8) and (9), readily yield

$$T = \frac{1-r^2}{4} + \frac{R^2-1}{4 \ln R} \ln r, \quad (12)$$

$$\psi = Ra\left[\frac{R^2}{16} r^{-1} - \frac{R^2-1}{16} r - \frac{r^3}{16} + \frac{R^2-1}{8 \ln R} r \ln r\right] \sin \phi. \quad (13)$$

It can be easily seen from these solutions that under the effect of uniform heating, the fluid temperature is non-uniformly increased to attain a maximum value along the radius

$$r_{\max} = \sqrt{[(R^2-1)/2 \ln R]}, \quad (14)$$

which separates the fluid into two layers, namely the inner and the outer layers. In the upper part of the cavity, the outer layer is bottom-heated, therefore potentially unstable, while the inner layer is top-heated and stable. The situation is reversed in the lower part of the cavity. In the middle of the cavity ($\phi \approx \pi/2$) both layers are side-heated along the lines of maximum temperature where the fluid is buoyed upward to separate into two counter-rotating vortices. It should be noted that the occurrence of two counter-rotating vortices in each half cavity is characteristic of the geometry and boundary conditions considered here, namely a doubly-connected flow domain with both boundaries maintained at a fixed temperature.

As R is increased, it can be seen from equations (12) and (13) that the hot line is moved closer to the inner boundary and the outer circulation is dominating the inner one, so that, as can be expected, in the limit of $R \to \infty$, the maximum temperature is located at the center of the cavity and the flow pattern will consist of only one cell (in each half cavity). The opposite limit of $R \to 1$ corresponds to the case of an infinitely tall vertical slot (at $\phi \approx \pi/2$) where the flow field consists of two symmetrical counter-rotating circulations. In fact, in this latter case, it can be seen from the vorticity equation that both the velocity and temperature will have a similar profile, i.e. $V = Ra(T - \bar{T})$ where $\bar{T}$ is the average porous medium temperature. For $R > 1$, this symmetry is destroyed, but, interestingly enough, the velocity (at any given angular position) is found to be about the same along the inner and outer boundaries.

The boundary layer regime

At sufficiently high Rayleigh numbers, the flow will have a boundary layer-core structure in which the internally generated heat is transported upward mainly by convection, except in a thin layer along the boundary of the cavity where both convection and conduction are of importance and must be taken into consideration. It should be noted that this boundary layer-core structure is essentially of thermal origin. This is due to the fact that only the energy equations contain both the convection and diffusion terms while vorticity is locally created by a horizontal temperature gradient, and cannot diffuse or convect within the cavity. Consequently, at high Rayleigh numbers, the two dynamic boundary layers that are developed along the inner and outer cylinders will have a similar thickness as that of the two thermal boundary layers.

In establishing the dimensionless governing equations (5) and (6), we have implicitly chosen the length, velocity and temperature scales that are characteristic of the pseudo conduction regime only. To describe the flow regime at high Rayleigh numbers, an appropriate scaling must explicitly show that, in the core region, the convection term is balanced by the source term, while it is balanced by the diffusion term in the boundary layers. Let us now designate by $\Delta\psi^*$, ΔT^* and ΔL^* the new stream function, temperature and length scales, respectively. A balance of the convection and source terms of the energy equation in the core region then requires that

$$\Delta\psi^* \sim (\Delta T^*)^{-1}, \quad (15a)$$

while a balance of the convection and diffusion terms in the boundary layers implies

$$\Delta\psi^* \sim (\Delta L^*)^{-1}. \quad (15b)$$

Finally, for vorticity to be generated within the boundary layers we must have

$$\Delta\psi^* \sim Ra\, \Delta L^* \Delta T^*. \quad (15c)$$

From these relations, we then find that the appropriate scaling is

$$\Delta L^* = \Delta T^* = Ra^{-1/3}, \quad (16a)$$

and

$$\Delta\psi^* = Ra^{1/3}. \tag{16b}$$

By renormalizing the energy and vorticity equations (5) and (6) according to these new scales and formally taking the limit $Ra \to \infty$, we finally obtain the following systems for the core region and boundary layers, respectively.

(1) In the core region

$$\frac{\partial\psi^*}{r\partial\phi}\frac{\partial T^*}{\partial r} - \frac{\partial\psi^*}{\partial r}\frac{\partial T^*}{r\partial\phi} = 1, \tag{17}$$

$$\sin\phi\frac{\partial T^*}{\partial r} + \cos\phi\frac{\partial T^*}{r\partial\phi} = 0. \tag{18}$$

(2) In the boundary layers

$$\frac{\partial\psi^*}{r_w\partial\phi}\frac{\partial T^*}{\partial\eta} - \frac{\partial\psi^*}{\partial\eta}\frac{\partial T^*}{r_w\partial\phi} - \frac{\partial^2 T^*}{\partial\eta^2} = 0, \tag{19}$$

$$\sin\phi\frac{\partial T^*}{\partial\eta} - \frac{\partial^2\psi^*}{\partial\eta^2} = 0, \tag{20}$$

where $\psi^* = \psi/\Delta\psi^*$, $T^* = T/\Delta T^*$ and η is the stretched variable defined as

$$\eta = Ra^{1/3}(r - r_w), \tag{21}$$

with $r_w = 1$ and R for the inner and outer boundary layers, respectively.

From a preliminary analysis of the above equations, it can be shown that in the core region, the fluid temperature varies only in the vertical direction and the internally generated heat is convected upward with a velocity just equal to the inverse of the vertical temperature gradient. After reaching the top of the cavity, the heated fluid that has been transported from the core region will flow downward along the two boundary layers adjacent to the inner and outer cylinders. As the thickness of these layers would increase downstream, the temperature gradient, and therefore heat loss, should be strongest in the upper part of the annulus. Finally, as indicated by the scaling analysis, the boundary layer thickness will decrease as $Ra^{-1/3}$ while the heat transfer rate and fluid velocity near the cavity walls increase as $Ra^{1/3}$. It is of interest to note that this increase of the heat transfer rate is quite fast in comparison with that of a heat generating fluid in a continuous medium where, as shown by Bergholz [1] for the case of a rectangular cavity, the Nusselt number only increases as $Ra^{1/5}$.

NUMERICAL RESULTS

In this section, numerical solutions will be presented of the governing equations (5) and (6) under the boundary conditions (8) and (9). To obtain the temperature distribution, an alternating direction implicit method (ADI) was employed, with a maximum mesh size of 36×36, and a time step of 10^{-3}. The computational method involved differs slightly from that used by Mallison and de Vahl Davis [10]. The first and second derivations are approximated by central differences and the time derivatives by a first-order forward difference. The finite-difference expression of the energy equation is written in conservative form for the advective term in order to preserve the conservative property. To determine the stream function, the elliptic equation (5) was solved by the method of successive overrelaxation (SOR), with a relaxation factor of 1.8. The iterative procedure was repeated until the maximum change in the stream function was less than 5×10^{-4}. Once the velocity and temperature fields were determined, the local heat flux was calculated with a three-point difference formula of second-order accuracy; the overall heat transfer was next evaluated using Simpson's rule for numerical integration. For all the cases presented below, the energy balance [equation (24)] was satisfied to within 2%.

Due to the possible formation of Bénard's cells at the locations adjacent to the top of the outer cylinder ($\phi = 0, r = R$) and bottom of the inner one ($\phi = \pi, r = 1$) tests have been conducted to study the influence of initial conditions on the numerical results. It has been found that, in the range of the parameters considered in the present study, the solutions were independent of the initial temperature and velocity fields. It must also be mentioned that, in the case of a saturated porous medium bounded by two concentric, horizontal, isothermal cylinders, Caltagirone [11] has demonstrated experimentally and numerically the existence of a fluctuating three-dimensional (3-D) convection when the Rayleigh number was above a critical value. Of course, such instabilities can not be observed in the present 2-D model.

Isotherms and streamlines

Numerical results for various radius ratios and Rayleigh numbers are shown in Figs. 2(a)–(d) where the streamlines are presented on the right half of the cavity and the isotherms on the left half. In all these graphs, the increments between adjacent isotherms and streamlines are $\delta T = T_{cmax}/5$ and $\delta\psi = (\psi_{max} - \psi_{min})/8$, respectively. ($\psi_{max}$ and ψ_{min} are the values of the stream function at the centers of the clockwise and counterclockwise vortices, respectively; T_{cmax} is the maximum temperature in pure conduction.)

Figure 2(a), with $R = 2$ and $Ra = 50$, represents the pseudo conduction regime, with two counter-rotating crescent eddies, and almost concentric circular isotherms. The effect of increasing Ra, as can be seen from the sequence of Figs. 2(a) and (c), is to push the outer vortex center into the upper half of the cavity where the fluid penetrates more and more into the inner stable layer. On the other hand, the inner cell is squeezed at the top of the cavity while extending into the outer layer in the lower part of the cavity. As a consequence of the fluid circulation, more heat is transported upward, and a larger difference of temperature is observed between the upper and lower parts of the annulus. At sufficiently high Rayleigh numbers, e.g. $Ra > 2000$ and $R = 2$, the flow pattern develops into a core-boundary layer structure as described in the previous section.

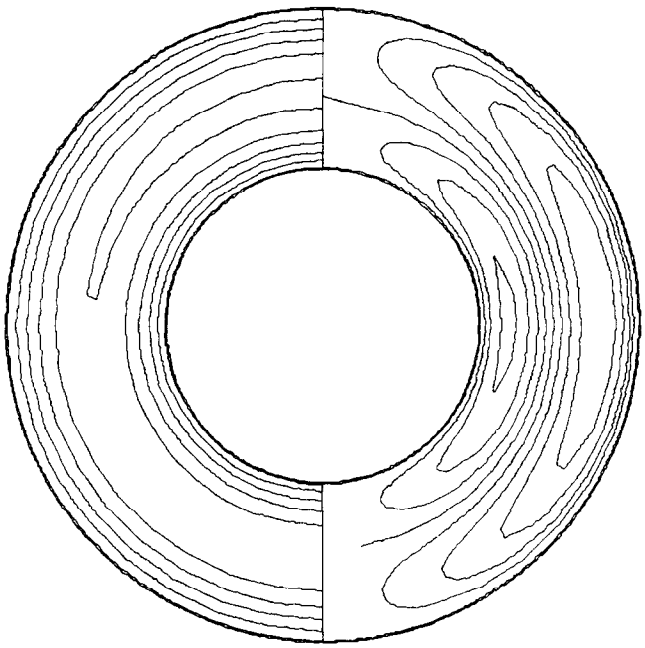

FIG. 2(a). Streamlines and isotherms for $Ra = 50$, $R = 2$; $\psi_{max} = 0.476$ and $\psi_{min} = 0.320$.

Figures 2(b) and (d) show the effect of an increasing radius ratio. Qualitatively, the same trend is observed in the development of the flow pattern and isotherms as for an increasing Rayleigh number.

Velocity and temperature distribution

The vertical velocities at the top ($\phi = 0$) and middle ($\phi = \pi/2$) of the annulus are shown in Figs. 3(a) and (b), respectively. Note that along the symmetry line ($\phi = 0$), the velocity vanishes at the point of separation of the two vortices. As Ra is increased, this separation point moves closer to the inner boundary and the upward flow (of the outer cell) becomes stronger than the downward flow of the inner cell. In the middle of the cavity, the effect of increasing Ra is more uniform across the annulus, and the upward and downward flows are of comparable intensity.

The temperature distributions across the annulus at

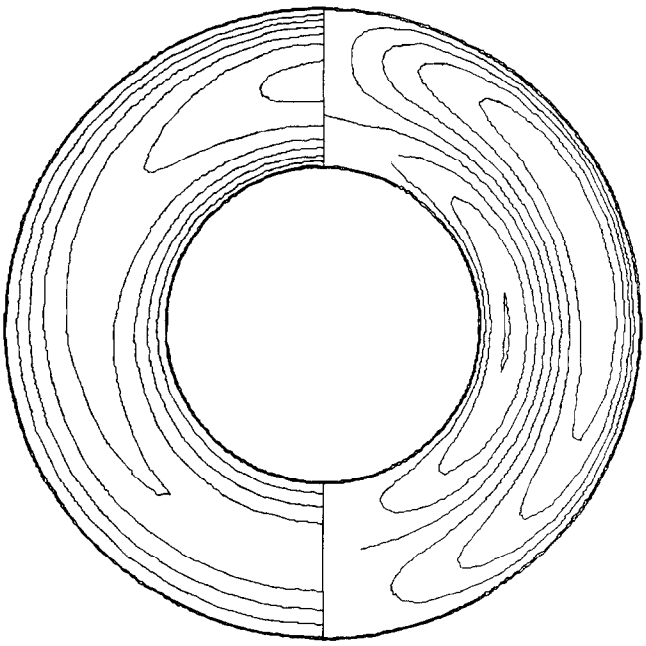

FIG. 2(b). Streamlines and isotherms for $Ra = 500$, $R = 2$; $\psi_{max} = 4.34$ and $\psi_{min} = -2.67$.

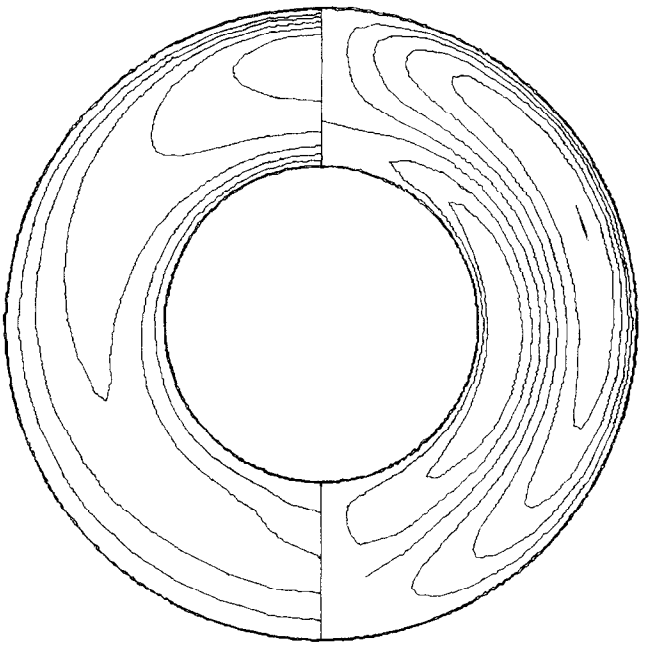

FIG. 2(c). Streamlines and isotherms for $Ra = 2000$, $R = 2$; $\psi_{max} = 12.5$ and $\psi_{min} = -7.23$.

various angular positions are shown in Fig. 4. For comparison, the temperature of the pure conduction state is shown by the dotted line. From Fig. 4, we note that at any radial position the temperature decreases with increasing angular position (i.e. in the downward direction). More precisely, the temperature profile at $\phi = 0$ lies above the curve for pure conduction while the profiles at $\phi = \pi/2$ and π lie below that curve. This process of local heating and cooling results from the fact that if the convective motion travels in a direction of increasing temperature, it will bring cold fluid into a hotter region, acting apparently as a sink of energy. Conversely, if the convective flow travels in a direction of decreasing temperature, it will blow hot fluid into a colder region, bringing in an extra amount of heat to increase the temperature of that region. (In a closed cavity, the average intensities of these 'sources' and 'sinks' must cancel out, as convection just transports

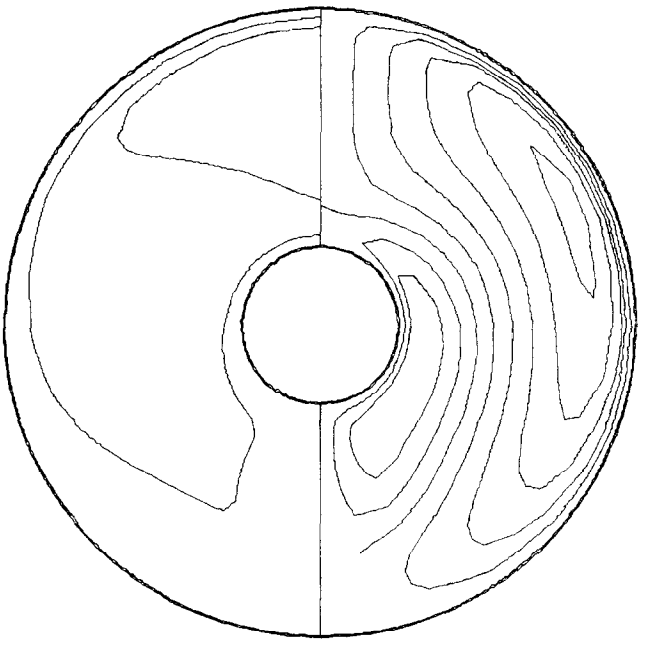

FIG. 2(d). Streamlines and isotherms for $Ra = 500$, $R = 4$; $\psi_{max} = 28.3$ and $\psi_{min} = -15.1$.

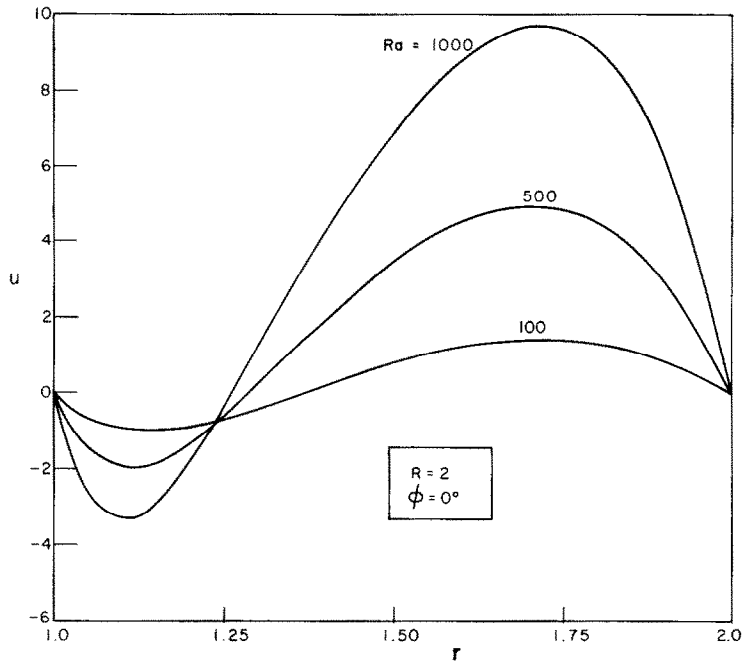

FIG. 3(a). Radial velocity profiles at $\phi = 0$ for $R = 2$ with Ra as a parameter.

energy from one point to another within the flow domain.)

The effect of convection on the distribution of temperature across the annulus is shown in Figs. 5(a) and (b). In the horizontal direction ($\phi = \pi/2$), the temperature is decreased everywhere, resulting in a smaller heat transfer rate at both the inner and outer boundaries. As Ra is increased, the temperature profile gradually changes to a rather flat curve, consisting of a horizontally uniform temperature core region and two boundary layers characterized by a strong temperature gradient.

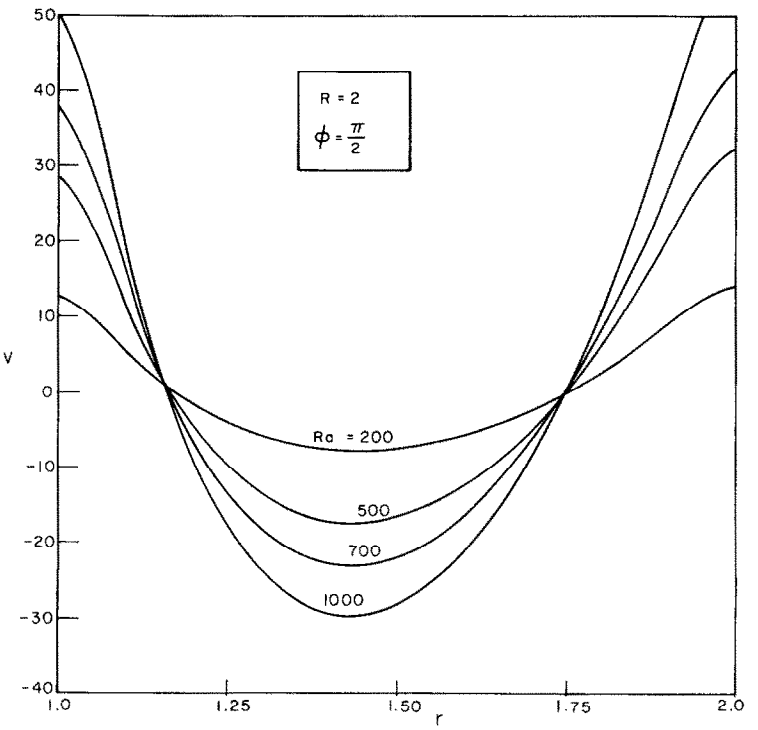

FIG. 3(b). Angular velocity profiles at $\phi = \pi/2$ for $R = 2$ with Ra as a parameter.

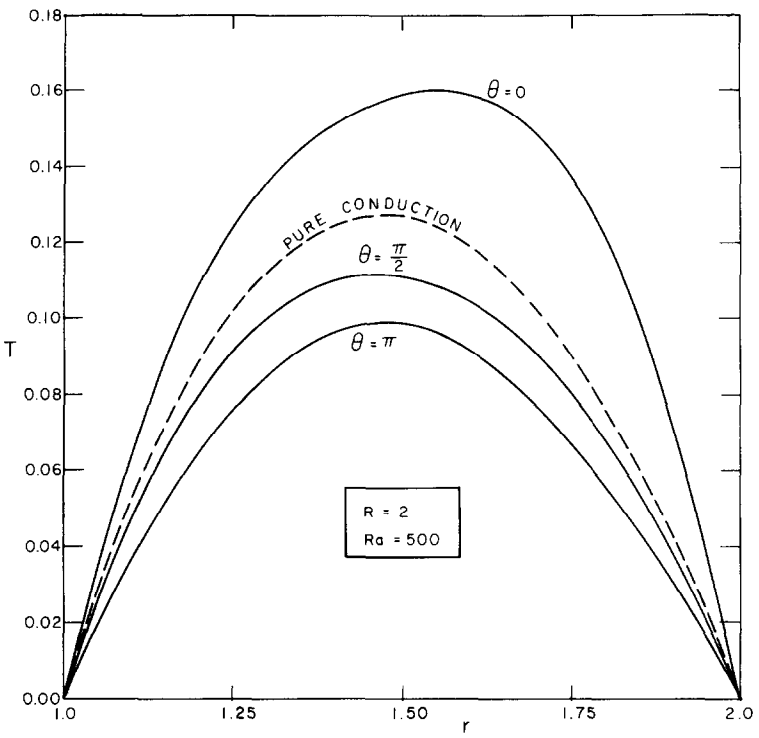

FIG. 4. Temperature profiles at different angular positions for $Ra = 500$ and $R = 2$.

Across the top of the annulus ($\phi = 0$), Fig. 5(b) shows that, as Ra is increased, the temperature gradients at both the inner and outer boundaries are increased. We also note that the hot spot (where temperature attains its maximum value) moves toward the outer cylinder, resulting in a greater heat loss across this boundary (compared to that at the inner one). At sufficiently high Rayleigh number, e.g. $Ra > 2000$, the temperature field develops into a stably stratified core (with an almost linear increase of temperature in the upward direction) and two thin layers in which the temperature sharply drops to the imposed value at the boundaries.

The maximum and average temperatures

A quantity of interest for design purposes is the maximum temperature, T_{max}, of the fluid near the top of the cavity. The effect of convection on the value of this maximum temperature is shown in Fig. 6(a) which shows that T_{max}, normalized by the maximum temperature for pure conduction, first increases with Ra to attain a maximum value before decreasing as $Ra^{-1/3}$ according to the dimensional analysis discussed in the previous section. The fact that T_{max} first increases with Ra can be understood by examining the temperature and velocity distributions shown in Figs. 3(a) and 4. From these figures, it appears that the flow at small Rayleigh numbers is almost everywhere in the direction of decreasing temperature, so that, as discussed in the previous paragraph, free convection increases the fluid temperature. However, due to the geometry under consideration, the velocity, in fact, does not change sign at the same point as the temperature gradient, resulting in a small region (between the points where the velocity and the temperature gradient vanish, respectively) in which the convective motion decreases the fluid temperature. As Ra is increased, this region becomes larger and larger and the overall effect of the fluid motion across the annulus is to reduce its temperature below that of pure conduction everywhere except in the boundary layers.

A more quantitative prediction of the initial increase of the fluid temperature with Ra can be obtained from a perturbation theory by determining the first-order (in Ra) term of the series solution for temperature as a correction to the pure conduction solution given by equation (12). These calculations, although straightforward, are rather cumbersome and will not be presented here.

Another quantity of interest is the average fluid temperature

$$\bar{T} = \frac{2}{\pi(R^2-1)} \int_0^{\pi} \int_1^{R} Tr \, dr \, d\phi, \qquad (22)$$

which represents the thermal energy (per unit volume) that is stored in the cavity. Figure 6(b) shows the variation of $\bar{T}$ in terms of Ra for various values of R. As can be expected, the ratio $\bar{T}/\bar{T}_c$ ($\bar{T}_c$ being the average temperature in the pure conduction state) is always less than 1, and monotonously decreases as Ra is increased, reflecting the fact that the overall effect of convection is to act as a more efficient energy transfer mechanism than conduction.

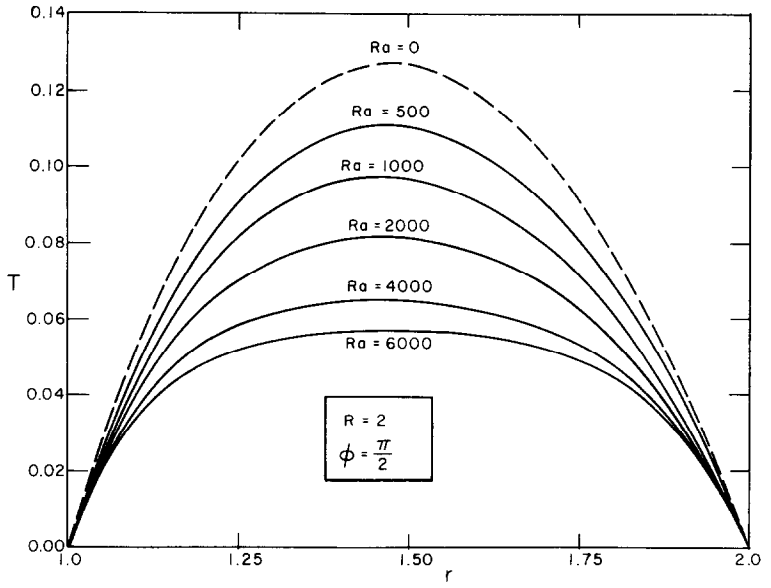

FIG. 5(a). Temperature profiles at $\phi = \pi/2$ for $R = 2$ with Ra as a parameter.

Heat transfer rates

The importance of heat transfer by convection can be described by the average heat flux across a unit angle. Since heat flows out of the cavity across both the inner and outer boundaries, we shall define an outward heat flux as positive, such that

$$Q_i = \frac{1}{\pi}\int_0^{\pi} \left.\frac{\partial T}{\partial r}\right|_{r=1} d\phi, \tag{23a}$$

and

$$Q_o = -\frac{R}{\pi}\int_0^{\pi} \left.\frac{\partial T}{\partial r}\right|_{r=R} d\phi, \tag{23b}$$

where Q_i and Q_o are the dimensionless heat fluxes across the inner and outer boundaries, respectively.

It should be noted that although Q_i and Q_o must change under the influence of convection, their sum just represents the total energy loss per unit angle and

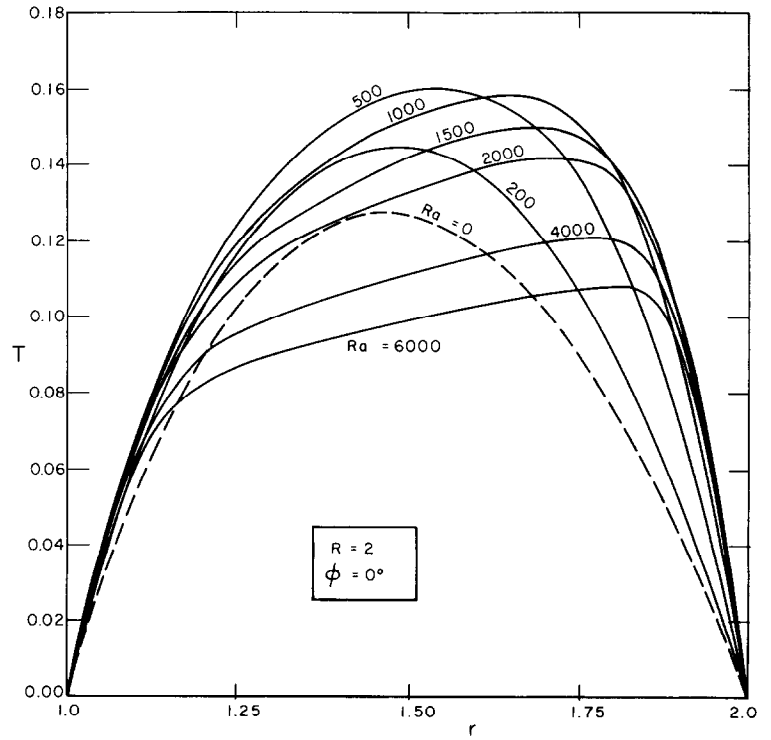

FIG. 5(b). Temperature profiles at $\phi = 0$ for $R = 2$ with Ra as a parameter.

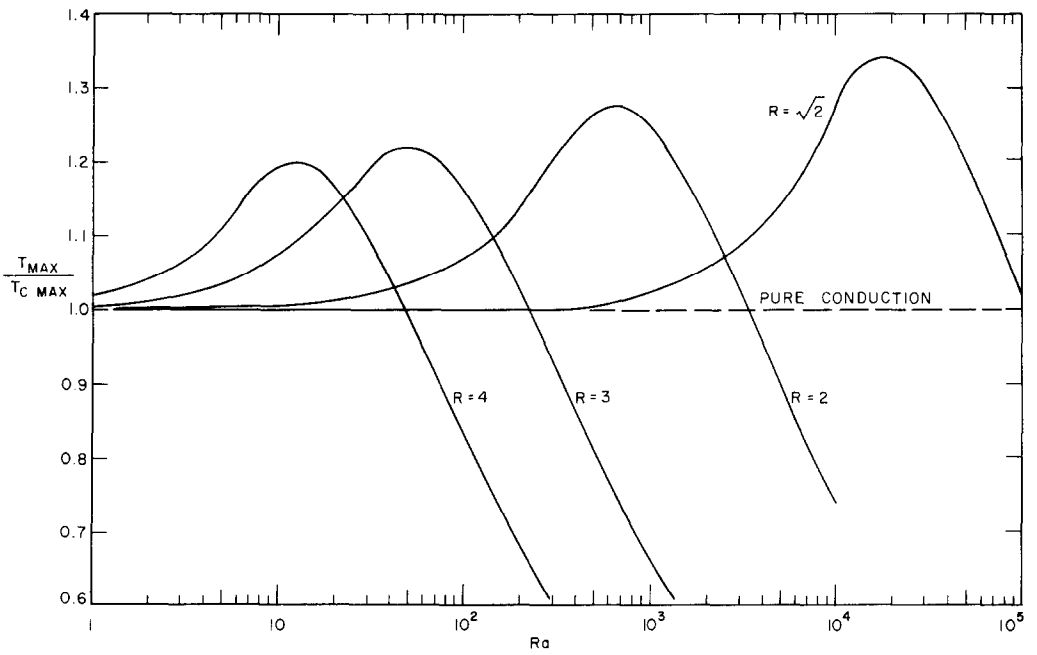

FIG. 6(a). Maximum temperature as a function of Ra and R.

(under steady-state conditions) must be equal to the rate of internal heat generation, i.e.

$$Q_i + Q_o = \frac{R^2 - 1}{2}. \tag{24}$$

The effect of convection on the heat transfer is shown in Fig. 7 where the heat fluxes Q_i and Q_o are given in terms of the Rayleigh number for various radius ratios R. For the values of R and Ra given in Fig. 7, Q_o and Q_i are an increasing and decreasing function of Ra, respectively. However, it should be noted that these functions must eventually attain some asymptotic values so that the system will not loose more energy than it can generate!

Finally, some remarks are in order about the well-known Nusselt number which is defined as

$$Nu = Q/\Delta T, \tag{25}$$

where ΔT is a characteristic temperature difference within the cavity. For the problem considered here we do not have a well-defined characteristic temperature difference as in the case of two concentric cylinders that are maintained at two different temperatures. As a consequence, it is difficult to justify a unique choice of

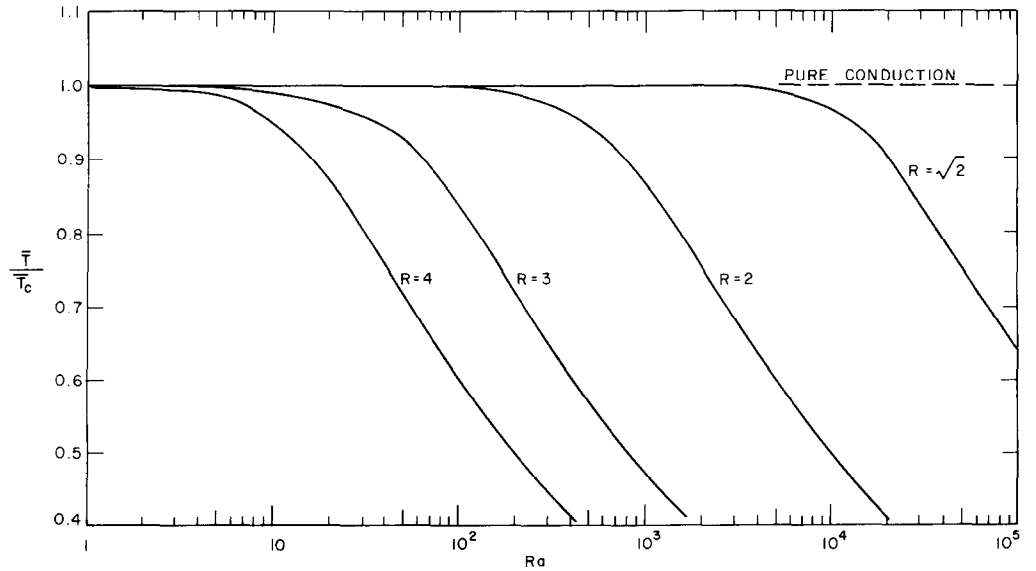

FIG. 6(b). Average temperature as a function of Ra and R.

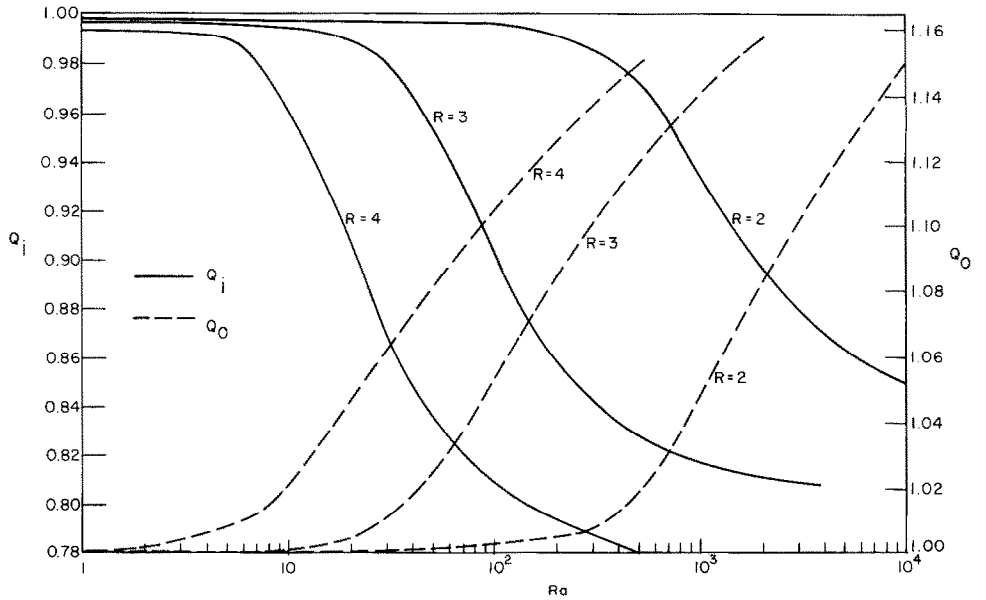

FIG. 7. Heat fluxes across the inner and outer cylinders as functions of Ra and R.

ΔT in the definition of the Nusselt number. For example, one could choose $\Delta T = T_{max}$, which is typical in the sense that, at low Rayleigh numbers, it is the temperature along the hot circle of radius r_{max} [see equation (14)]. However, as Ra is increased, this hot line is reduced to a hot spot in the top of the cavity and T_{max} then becomes less representative while the average temperature $\bar{T}$ might be more appropriate in defining a heat transfer coefficient. In any case, the Nusselt number can readily be determined from the above results for T_{max}, $\bar{T}$, and Q.

CONCLUSION

The problem of free convection in a horizontal porous layer with internal heat sources has been solved for a wide range of Rayleigh numbers ($0 < Ra < 10^4$) under the assumption of 2-D laminar Darcy flow.

For the geometry and boundary conditions considered in the present study, it should be noted that in the pseudo-conduction regime, the effect of an internal heat source is to heat up the core fluid, and to establish a more or less parabolic temperature profile across the annulus. The primary convective flow in each half cavity then consists of two counter-rotating vortices whose relative size and intensity depend essentially on the radius ratio R. As convection gets stronger, the temperature in the upper part of the annulus can be considerably increased. For example, when $R = 2$ and $Ra = 500$, the maximum temperature of the fluid is about 25% higher than the value obtained under the pure conduction state. At very high Rayleigh numbers, both analytical and numerical analyses reveal a flow structure consisting of a thermally stratified core region and two boundary layers with a thickness of the order of $Ra^{-1/3}$. Under the effect of convection, the fluid temperature then decreases as $Ra^{-1/3}$ while the heat transfer rate increases as $Ra^{1/3}$. Finally, it should be noted that the scope of this study is limited by the assumption of 2-D steady laminar flow, i.e. nothing can be said about the very possible development of various types of instabilities that could lead to an unsteady and/or 3-D flow within the range of Rayleigh numbers considered in the present study.

Acknowledgements—This work was supported by the National Research Council of Canada through grants NRC A-9201 and NRC A-4197.

REFERENCES

1. R. F. Bergholz, Natural convection of a heat generating fluid in a closed cavity, *J. Heat Transfer* **102,** 242–247 (1980).
2. L. de Socio, L. Misici and A. Polzonetti, Natural convection in heat generating fluids in cavities, 18th National Heat Transfer Conf., San Diego, ASME/AICHE Paper 78-HT-95 (1979).
3. A. Emara and F. Kulacki, A numerical investigation of thermal convection in a heat-generating fluid layer, *J. Heat Transfer* **102,** 531–537 (1980).
4. R. Kee, C. Landram and J. Miles, Natural convection of a heat generating fluid within closed vertical cylinders and spheres, *J. Heat Transfer* **98,** 55–61 (1976).
5. J. Nelsen, R. Douglass and D. Alexander, Natural convection in a spherical annulus filled with heat generating fluid, 7th Int. Heat Transfer Conf., München, Fed. Rep. of Germany, Paper NC9, pp. 171–176 (1982).
6. J. H. Min and F. A. Kulacki, Natural convection with volumetric energy sources in a fluid bounded by a spherical segment, 7th Int. Heat Transfer Conf., München, Fed. Rep. of Germany, Paper NC8, pp. 165–168 (1982).
7. R. D. Gasser and M. S. Kazimi, Onset of convection in a porous medium with internal heat generation, *J. Heat Transfer* **98,** 48–54 (1976).
8. M. Tveitereid, Thermal convection in a horizontal porous layer with internal heat generation, *Int. J. Heat Mass Transfer* **20,** 1045–1050 (1977).

9. C. W. Somerton, J. M. McDonough and I. Catton, Natural convection in a volumetrically heated porous layer, Winter Annual Meeting of A.S.M.E. HTs-Vol. 22, Heat transfer in porous media, Phoenix, Arizona, pp. 43–47 (1982).
10. G. D. Mallison and G. de Vahl Davis, The method of the false transient for the solution of coupled elliptic equations, *J. Comp. Phys.* **12**, 435–461 (1973).
11. J. P. Caltagirone, Thermoconvective instabilities in a porous medium bounded by two concentric horizontal cylinders, *J. Fluid Mech.* **76**, 337–362 (1976).
12. H. C. Brinkman, Calculation of the viscous force extended by a flowing fluid on a dense swarm of particles, *Appl. Scient. Res.* **A1**, 27–34 (1947).
13. M. Muskat, *The Flow of Homogeneous Fluids through Porous Media*. Edwards, Michigan (1946).
14. K. Vafai and C. L. Tien, Boundary and inertia effects on flow and heat transfer in porous media, *Int. J. Heat Mass Transfer* **24**, 195–203 (1981).

APPENDIX

ON THE VALIDITY OF DARCY'S LAW

It is well known that the empirical Darcy's law is valid only when the effects of inertial forces and vorticity diffusion near solid boundaries can be neglected. These effects were first considered by Brinkman [12] and Muskat [13] who respectively added a diffusion term and a quadratic term in Darcy's law to account for the viscous resistance due to the boundary and the resistance due to inertial forces. Strictly speaking, exact expressions of inertial and viscous forces have not been obtained, as the complex structure of pore channels still defines a rational description of fluid flow in a porous medium.

In a recent study, Vafai and Tien [14] have shown that the effects of a solid boundary and inertial forces on flow and heat transfer in porous media can be significant in highly permeable media, high Prandtl number fluids, large pressure gradients, and in the leading edge of the flow boundary layer. Using a local volume-averaging technique, these authors have shown that, in fact, these effects are characterized by two dimensionless parameters, namely the inertial and the boundary parameters which can be expressed in the following form:

$$\pi_i = nF\,Re\,\sqrt{Da}, \tag{A1}$$

$$\pi_d = Pr^2\,Da/n, \tag{A2}$$

where π_i is the inertial parameter, π_d the boundary parameter, n the porosity, Da the Darcy number, Pr the Prandtl number, and Re the Reynolds number based on the characteristic length of the flow domain. The coefficient F, which is to be determined empirically, is a function of the porous structure as well as the fluid velocity and flow geometry.

By solving the momentum and energy equations in which the effects of both vorticity diffusion and inertia were included, Vafai and Tien have found that the results obtained from Darcy's law are within an error of 10% or less if

$$\pi_i < 6 \times 10^{-3}, \tag{A3}$$

and

$$\pi_d < 1. \tag{A4}$$

Given equations (A1) and (A2), these conditions put the following limits on the Darcy and Reynolds numbers

$$Re < \frac{6 \times 10^{-3}}{nF\sqrt{Da}} \tag{A5}$$

and

$$Da < \frac{n}{Pr^2}, \tag{A6}$$

or, in terms of the characteristic velocity U' and characteristic length L'

$$U' < \frac{6 \times 10^{-3} \nu}{nF\sqrt{K}}, \tag{A7}$$

and

$$L' > Pr\,\sqrt{(K/n)}. \tag{A8}$$

It should be noted that while this latter condition (A8) can be easily satisfied, except for very high Prandtl number ($Pr \simeq 10^3$), the first condition (A7) is more restrictive than the commonly evoked condition that the Reynolds number Re^* based on the pore diameter d' be smaller than 1. In fact, condition (A7) implies that

$$Re^* < \frac{6 \times 10^{-3} d'}{nF\sqrt{K}}. \tag{A9}$$

As an example, let us consider the case of a water-saturated porous medium [14] with $n \simeq 0.98$, $F \simeq 7 \times 10^{-2}$, $K = 10^{-6}$ m^2, $\nu = 1.5 \times 10^{-6}$ m^2 s^{-1}, and $Pr = 11.5$. Substituting these values into equations (A7)–(A9) we readily obtain

$$U' < 10^{-4}\ \text{m s}^{-1}, \tag{A10}$$

$$L' > 10^{-2}\ \text{m}, \tag{A11}$$

and

$$Re^* < 10^{-2} d'. \tag{A12}$$

Thus for a cavity with, for instance, a characteristic length $L' = r_i' = 0$(1 m), the above equations will be satisfied even for the highest Rayleigh number considered in the present study, i.e. $Ra = 10^4$, with a radius ratio $R = 2$, as the maximum velocity was found to be less than 0.35×10^{-4} m s^{-1}. Furthermore, the corresponding characteristic temperature difference $\Delta T = O(1°C)$ is small enough to warrant the validity of the Boussinesq approximation.

CONVECTION NATURELLE ENTRE DES CYLINDRES COAXIAUX, HORIZONTAUX, REMPLIS PAR UN MILIEU POREUX AVEC UNE GENERATION INTERNE DE CHALEUR

Résumé—On étudie numériquement la convection naturelle dans une couche annulaire avec génération interne de chaleur. Aux faibles nombres de Rayleigh, un profil plus ou moins parabolique de température est établi à travers l'anneau, avec deux tourbillons contra-rotatifs dans chaque demi-cavité. Sous l'effet de la convection faible ou modérée, la température maximale dans le milieu poreux peut être considérablement plus grande que celle induite par conduction pure. Aux grands nombres de Rayleigh, les solutions analytiques et numériques révèlent une structure d'écoulement stratifié puis deux couches limites avec une épaisseur, et le flux de chaleur est respectivement de l'ordre de $Ra^{-1/3}$ et $Ra^{1/3}$.

FREIE KONVEKTION IM ZWISCHENRAUM VON HORIZONTALEN KONZENTRISCHEN ZYLINDERN, DER VON EINEM PORÖSEN MEDIUM MIT INNEREN WÄRMEQUELLEN AUSGEFÜLLT IST

Zusammenfassung—Das Problem der freien Konvektion in einer ringförmigen porösen Schicht mit inneren Wärmequellen wird numerisch untersucht. Bei kleinen Rayleigh-Zahlen stellt sich mehr oder weniger ein parabolisches Temperaturprofil quer über die Ringbreite ein, das zu zwei gegensinnig rotierenden Wirbeln in jeder Ringhälfte führt. Schon bei schwacher und mäßiger Konvektion kann die maximale Temperatur im porösen Medium beträchtlich höher als bei reiner Wärmeleitung sein. Bei großen Rayleigh-Zahlen ergeben sowohl analytische wie auch numerische Berechnungen eine Strömungsform, die aus einem thermisch geschichteten Kern und zwei Grenzschichten besteht, deren Dicke und deren Wärmeübergangskoeffizient proportional zu $Ra^{-1/3}$ bzw. $Ra^{1/3}$ sind.

ЕСТЕСТВЕННАЯ КОНВЕКЦИЯ В ПОРИСТОМ СЛОЕ МЕЖДУ ГОРИЗОНТАЛЬНЫМИ КОНЦЕНТРИЧЕСКИМИ ЦИЛИНДРАМИ С ВНУТРЕННИМ ИСТОЧНИКОМ ТЕПЛА

Аннотация—Численно исследуется естественная конвекция в кольцевом пористом слое с внутренним тепловыделением. При малых значениях числа Релея устанавливается более или менее параболический температурный профиль поперек кольцевого канала, в результате чего в каждой половине полости возникают два противоположно вращающихся вихря. Из-за влияния слабой и умеренной конвекции максимальное значение температуры в пористой среде может намного превышать значение, определяемое чистой теплопроводностью. Аналитический и численный анализ показывает, что при больших значениях числа Релея структура потока состоит из термически стратифицированного ядра и двух пограничных слоев толщиной порядка $Ra^{-1/3}$ и интенсивностью теплопереноса порядка $Ra^{1/3}$.